JOURNAL OF VIROLOGY, Apr. 2008, p. 4072–4081 Vol. 82, No. 8
0022-538X/08/$08.00+0 doi:10.1128/JVI.02319-07

Identification of a Hydrophobic Domain of HA2 Essential to Morphogenesis of *Helicoverpa armigera* Nucleopolyhedrovirus▽

Qian Wang,[1,2] Yun Wang,[1] Changyong Liang,[1] Jianhua Song,[1] and Xinwen Chen[1]*

State Key Laboratory of Virology, Wuhan Institute of Virology, Chinese Academy of Sciences, Wuhan 430071,[1] and Department of Biochemistry & Molecular Biology, Nanjing Medical University, Nanjing,[2] China

Received 25 October 2007/Accepted 21 January 2008

The HA2 protein of the *Helicoverpa armigera* single-nucleocapsid nucleopolyhedrovirus (HearNPV) is a WASP homology protein capable of nucleating branched actin filaments in the presence of the Arp2/3 complex in vitro. To determine the role of *ha2* in the HearNPV life cycle, *ha2* knockout and *ha2* repair bacmids were constructed. Transfection and infection analysis demonstrated that the *ha2* null bacmid was unable to produce infectious budded virus (BV), while the repair bacmid rescued the defect. In vitro analysis demonstrated that the WCA domain of HA2 accelerates Arp2/3-mediated actin assembly and is indispensable to the function of HA2. However, analysis of the repaired recombinant with a series of truncated *ha2* mutants demonstrated that the WCA domain was essential but not enough to yield infectious virions, and a hydrophobic domain (H domain) consisting of amino acids (aa) 167 to 193 played a pivotal role in the production of BV. Subcellular localization analysis with enhanced green fluorescent protein fusions showed that the H domain functioned as a nuclear localization signal. In addition, deletion of the C terminus of the *ha2* product, a phosphatidylinositol 4-kinase homolog, dramatically decreased the viral titer, while deletion of 128 aa from the N terminus did not affect HA2 function.

Rearrangement of the actin cytoskeleton in response to viral infection has been observed for many viruses (8). Since Volkman et al. first demonstrated that microfilaments are involved in the production of budded virions (BV) of *Autographa californica* nucleopolyhedrovirus (AcMNPV) (26), all evidence to date indicates that nuclear F-actin is essential for nucleocapsid morphogenesis of nucleopolyhedroviruses (20, 25).

AcMNPV can induce sequential rearrangement and nuclear assembly of actin in infected cells (3). It has been reported that monomeric G-actin accumulated within the nuclei of AcMNPV-infected cells during the early stages of infection and that expression of six AcMNPV early genes (*ie-1*, *pe38*, *he65*, Ac*004*, Ac*102*, and Ac*152*) was sufficient for this to occur (19). The dynamic nuclear actin was polymerized by the Arp2/3 complex and a Wiskott-Aldrich syndrome protein (WASP) homolog, such as P78/83 of AcMNPV (9, 17) and HA2 of *Helicoverpa armigera* NPV (HearNPV) (18, 28), during baculovirus infection. Nuclear F-actin assembly by P78/83 and the Arp2/3 complex was essential for viral progeny production (9).

The overall arrangement of baculoviral WASP exhibits the same proline-rich, WH2 (verprolin homolog; W), cofilin homology (C), and acidic (A) motifs as its counterparts, the WASP family proteins (4, 17, 18). The WCA domain of AcMNPV P78/83 stimulates actin polymerization into Y branches with the Arp2/3 complex in vitro and also plays an essential role in AcMNPV replication (9). Although all WASPs and WASP family verprolin-homologous proteins (WAVEs) have a WCA region, which associates with actin and the Arp2/3 complex and is critical for Arp2/3 complex-induced actin polymerization, there still exist differences in the potencies of WCA regions from WASPs and WAVEs in Arp2/3 complex activation (23, 29). On the other hand, the *ha2* product shares very low homology with other WASPs (17). Besides the conserved motifs, the N and C termini of HA2 are highly diverse. Sequence analysis indicated that the N-terminal 128 amino acids (aa) of HA2 have no homolog in GenBank, while the C-terminal 152 aa contain a phosphatidylinositol 4-kinase (PtdIns 4-kinase)-homologous domain. It has been reported that PtdIns 4-kinase is involved in normal actin cytoskeleton organization (1). Thus, it is of great benefit to analyze the functions of the different domains of HA2.

In this study, we generated an *ha2* knockout bacmid via homologous recombination to determine the role of HA2 in viral replication. Our results showed that *ha2* was an essential gene necessary for virus propagation. By the repair of a series of mutants of *ha2*, we demonstrated that those truncated *ha2* mutants which covered the WCA domain could yield infectious virions. Further investigation described the activity of the HA2 WCA region, which could activate the Arp2/3 complex in vitro. Moreover, by combining the results of the recombinant viruses and the subcellular localization of the different fragments, a new hydrophobic domain (aa 167 to 193) was characterized.

MATERIALS AND METHODS

Cells, viruses, bacterial strains, and plasmids. *Helicoverpa zea* (BCIRL-Hz-AM1 and Hz-AM1) cells were maintained at 28°C in Grace's medium supplemented with 10% fetal bovine serum (Gibco BRL). HearNPV G4, whose genome has been sequenced entirely (4), and recombinant vHa-eGFP (18) and HaBacHZ8 (27) were propagated in Hz-AM1 cells before use.

BW25113(pKD46)(HaBacHZ8) was constructed and preserved in our lab (11); this strain contained a HearNPV bacterial artificial chromosome (HaBacmid) and could express λ phage red recombinase. Plasmid pKD3 contained the chloramphenicol resistance gene (*cat*) (kindly provided by B. L. Wanner of Purdue University) (6).

Generation of *ha2* knockout HearNPV bacmid. Using the λ red recombinant system, an *ha2* knockout HearNPV was generated through homologous recom-

* Corresponding author. Mailing address: State Key Laboratory of Virology, Wuhan Institute of Virology, Chinese Academy of Sciences, Wuhan 430071, People's Republic of China. Phone and fax: 86-027-87199106. E-mail: chenxw@pentium.whiov.ac.cn.

▽ Published ahead of print on 30 January 2008.

TABLE 1. Oligonucleotides used for this study

Name	Sequence (5′ to 3′)[a]
CATU	TGT AGG CTG GAG CTG CTT C
CATD	ATA TGA ATA TCC TCC T TAG
PR1	CCG *GTA TAC* (Bst1107I) ACG TCA AGA TGC CCA AAG
PR2	CGG *GAA TTC* (EcoRI) TAT TGC GAA TCG CAA TGG
A1	CG*GAATTC* (EcoRI) ATGGTTCAACTG CAAAGTGTT
A2	CG*GAATTC* (EcoRI) ATGCCGCAAAC ACTTATGCCG
A3	CG*GAATTC* (EcoRI) ATGTTAATAGAA GATATAGTA
A4	CG*GAATTC* (EcoRI) ATGGATCCACGT ACCGAATTG
A5	CG*GAATTC* (EcoRI) ATGCAACAGCA GCGAGCCAGC
A6	CG*GAATTC* (EcoRI) ATGTCATTACCA TTAATAGAA
B1	CC*TCTAGA* (XhoI) TTAAACTTGCGAT TCAGTTGA
B2	CCC*TCTAGA* (XhoI) TTTTAAAACTTG CCGAGT
B3	CCC*TCTAGA* (XhoI) TTCGTCGTCGGT CCACCC
egfp1 forward	CCG *GGG CCC* (SmaI) ATG GTG AGC AAG GGC GAG GAG
egfp1 reverse	GCG *GGT ACC* (KpnI) CTT GTA CAG CTC GTC CAT
M 13 forward	GTTTTCCCAGTCACGAC
egfp2 forward	CCA *GGA TCC* (BamHI) AAC CAT GGT GAG CAA GGG CG
egfp2 reverse	GCG *GGA TCC* (EcoRI) TTA CTT GTA CAG CTC GTC CA
HP1	GAT CCA CGT ACC GAA TTG ATG GAA CAA ATA CAG AAA GGA ATG TAG GCT GGA GCT GCT TC
HP2	TTA AAC TTG CGA TTC AGT TGA CAT CGT CAA TTT GTA ACT CAT CCA TAT GAA TAT CCT CCT TAG
477F	GCC GCC GCC TCC TCC GCC ACC
643R	GCC ATC GGC GGG TTT TGA TAC
p10F	ATG TCA CAA AAC ATT CTA
p10R	TCA TTT TTT ATT GGA CAC
vp39F	ATG GCC CTT GTT ACC GTG
vp39R	TTA TCG TCC TGT GCT GAT

[a] Restriction enzyme sites are indicated in italics.

TABLE 2. Donor plasmids and oligonucleotides used for this study

Donor plasmid	Fragment (aa position)	Primers
pFBGpha2-ha2	WT (1–413)	A1/B1
pFBGpha2-C129	C129 (129–413)	A2/B1
pFBGpha2-C170	C170 (170–413)	A3/B1
pFBGpha2-C194	C194 (194–413)	A4/B1
pFBGpha2-C261	C261 (261–413)	A5/B1
pFBGpha2-N193	N193 (1–193)	A1/B2
pFBGpha2-N260	N260 (1–260)	A1/B3
pFBGpha2-PWCA	PWCA (129–260)	A2/B3
pFBGpha2-HWCA	HWCA (167–260)	A6/B3
pFBGpha2-WCA	WCA (194–260)	A4/B3

bination in *Escherichia coli* as previously described (6, 11). First, a linear fragment for generating *ha2*-replaced recombinant HearNPV was obtained by the PCR method. Primers used for PCR were HP1 and HP2. Both primers were made up of two parts. The first 40 bp was homologous to the 3′ region of *ha2* (HearNPV nucleotides [nt] 738 to 1402), and the other 19 bp was homologous to *cat* (chloramphenicol acetyltransferase gene) (Table 1). The resulting linear 1.1-kb fragment, containing the *cat* gene cassette and the *ha2* flanking region, was PCR amplified from plasmid pKD3, gel purified, and suspended in distilled water. *E. coli* BW25113 competent cells were electroporated with the 1.1-kb fragment. The electroporated cells were incubated at 37°C for 4 h in 1 ml of SOC medium and spread onto an LB plate containing 50 μg/ml kanamycin and 25 μg/ml chloramphenicol (15). The plates were incubated at 37°C for 2 days, and colonies resistant to kanamycin and chloramphenicol were selected and confirmed by PCR.

Six different primer pairs (Table 1) were used to confirm that the 3′ region of *ha2* had been deleted from the *ha2* locus of the HearNPV bacmid genome. Primer pairs CATU/B1 and CATU/CATD were used to detect the correct insertion of the *CAT* gene cassette. Primer pairs A4/B2 and A5/B1 were used to confirm the loss of the *ha2* coding region. Primer pairs A1/CATD and A4/B1 were used to examine the recombination junctions of the upstream and downstream flanking regions. One recombinant bacmid with both correct PCR confirmations was selected and named HaΔha2.

Construction of donor plasmids. To generate an *ha2* repair bacmid, transfer plasmids were constructed for transposition into the *polh* locus of the *ha2* knockout bacmid according to the Bac-to-Bac protocol (Invitrogen). First, the pFastBac Dual transfer plasmid (Invitrogen Life Technologies), containing two multicloning regions, was digested with Bst1107I and EcoRI to remove the *polh* promoter and replaced with the native *ha2* promoter (nt 1992 to 2082), which was amplified from the HearNPV G4 genomic template by using primers PR1 and PR2. A copy of the enhanced green fluorescent protein gene (*egfp*), which was PCR amplified from pEGFP-N1 using primers egfp1 forward and egfp1 reverse, was inserted into the p10 multicloning region of the altered pFastBac Dual plasmid, and the resulting construct was named pFBGpha2. Finally, *ha2* and a series of truncated *ha2* fragments were inserted between EcoRI and XhoI sites under the control of the *ha2* promoter. All of these fragments were obtained by the PCR method with the primer pairs listed in Tables 1 and 2.

Construction of knockout and repair HearNPV bacmids containing *ha2* promoter and *egfp*. HearNPV bacmids containing the *ha2* promoter and the *egfp* cassette were generated by Tn7-mediated transposition as previously described (15). To prepare bacmids for transposition, the helper plasmid pMON7124, which confers resistance to tetracycline and encodes a transposase, was transformed into DH10B cells harboring an *ha2* knockout bacmid, HaΔha2. These cells were then transformed with donor plasmid pFBGpha2-X ("X" represents empty plasmid or wild-type [WT] or truncated *ha2* fragments), incubated at 37°C for 4 h in 1 ml of SOC medium, and placed onto agar medium containing 50 μg/ml of kanamycin, 7 μg/ml of gentamicin, 10 μg/ml of tetracycline, 100 μg/ml of X-Gal (5-bromo-4-chloro-3-indolyl-β-D-galactopyranoside), and 40 μg/ml of IPTG (isopropyl-β-D-thiogalactopyranoside). Primers gfp1 forward and M13 forward were used to confirm the phenotypes of recombinant bacmids by PCR.

The correct bacmid constructs were then electroporated back into *E. coli* DH10B cells and screened for tetracycline sensitivity to ensure that the isolated bacmids were free of helper plasmid artifacts. Equimolar amounts of purified bacmid DNA were transfected into Hz-AM1 cells (5×10^5) by use of a cationic liposome method. Transfection events were confirmed by *egfp* expression in bacmid DNA-transfected Hz-AM1 cells.

DNA replication assay. To assess viral DNA replication, a quantitative real-time PCR assay was performed as previously described (24). To prepare total DNA for analysis, 5×10^5 Hz-AM1 cells were transfected with 2.0 μg of bacmid DNA. At selected time points, cells were harvested in 1 ml phosphate-buffered saline (PBS), lysed in 500 μl cell lysis buffer (10 mM Tris, pH 8.0, 100 mM EDTA, 20 μg/ml RNase A, 0.5% sodium dodecyl sulfate), incubated for 30 min at 37°C before the addition of 100 μg/ml of proteinase K, and incubated overnight at 56°C. Total DNA was phenol extracted, ethanol precipitated, and suspended in 300 μl of water. Prior to PCR, 10 μl of total DNA from each time point was digested with 10 units of DpnI restriction enzyme (Fermentas) for 24 h in a 50-μl total reaction volume. Quantitative PCR was performed with 1 μl of digested DNA added to SYBR green real-time PCR master mix (Toyobo) according to the manufacturer's instructions and was analyzed on an Opticon sequence detection system under the following conditions: 50°C for 2 min, 95°C for 2 min, and 45 cycles of 95°C for 30 s and 60°C for 30 s, with a 500 nM concentration of each primer (477F and 643R). Cycle threshold (C_T) values were determined by automated threshold analysis using the Opticon software. Dissociation curves were recorded after each run.

Transcriptional activity assays. Total RNA was extracted from HaΔha2-eGFP- and HaΔha2-ha2-transfected Hz-AM1 cells by using RNAzol according

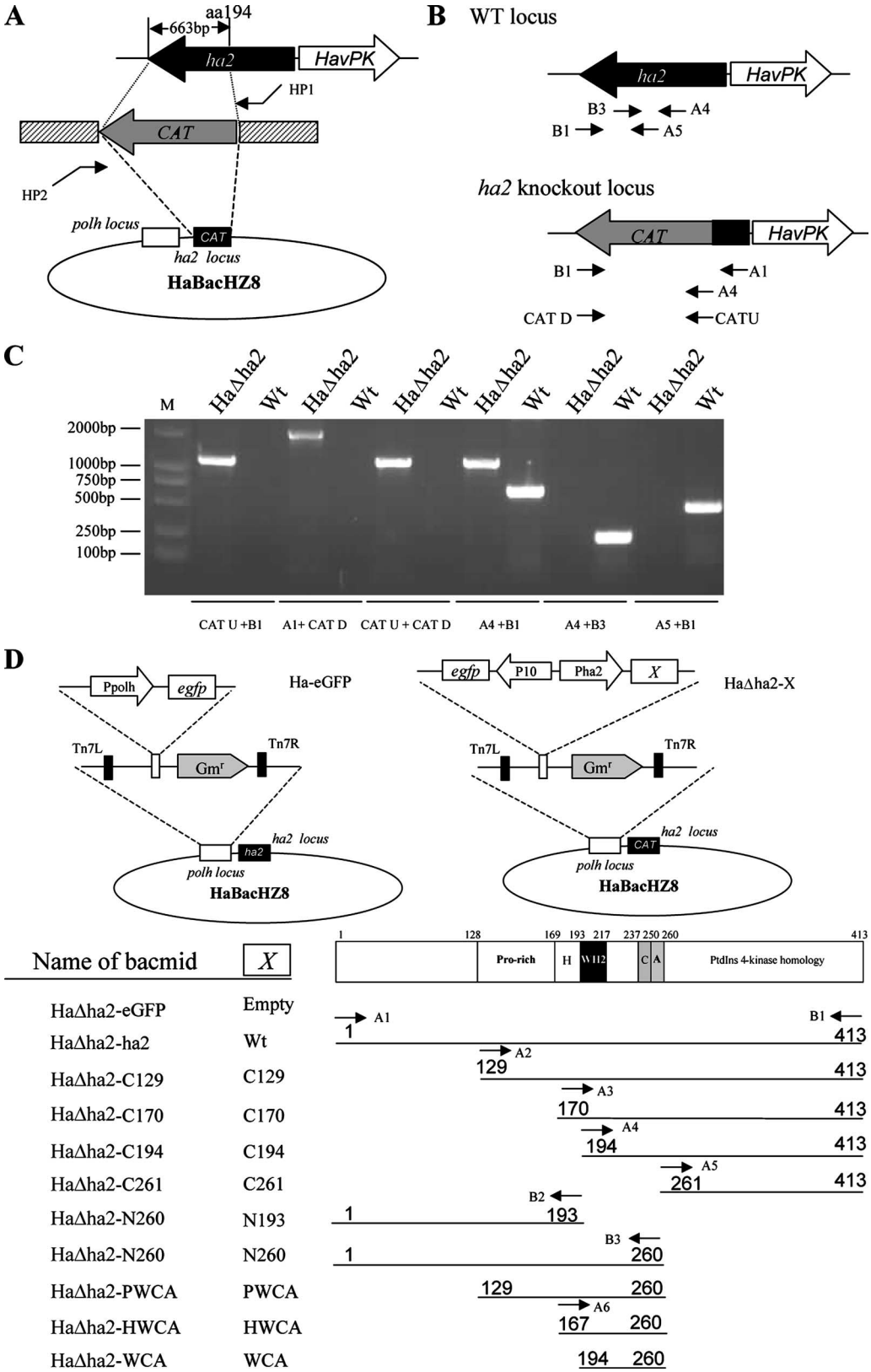

FIG. 1. Generation of recombinant bacmids. (A) Schematic diagram of construction of an *ha2* knockout bacmid containing a deletion of the HearNPV *ha2* gene by recombination in *E. coli*. A 663-bp portion of the *ha2* open reading frame was deleted and replaced with the chloramphenicol resistance gene (*cat*). (B) Positions of primer pairs used in analysis of the WT locus and *ha2* knockout locus to confirm the deletion of the *ha2* open reading frame and the correct insertion of the *cat* cassette. Primers are indicated by arrows. (C) Confirmation by PCR analysis of the presence or absence of sequence modifications in HaΔha2 and Ha-WT. The virus analyzed is shown above each lane, and the primer pairs used

to the supplier's protocol (Invitrogen). For detection of HearNPV gene expression, the RNA was pretreated for 30 min with RNase-free DNase (Promega) at 0.1 U/μg RNA. Reverse transcription (RT) reactions were carried out using 1 to 2 μg of DNase-treated RNA as the template, a random primer (Promega) as the primer, and Moloney murine leukemia virus reverse transcriptase (Promega). The RT reaction mix was incubated sequentially at 42°C for 60 min and 70°C for 15 min. The reaction was stopped by heating to 95°C for 5 min, 0.5 μl of RNase H (Promega) was added, and the reaction mix was incubated at 37°C for an additional 30 min. Afterward, the cDNA was stored at −80°C.

PCRs using KOD Plus DNA polymerase (Toyobo) were carried out using cDNAs as templates. To detect specific transcripts, the following forward and reverse primers were used in the PCRs: p10F and p10R for the *p10* gene (264-bp product) and vp39F and vp39R for the *vp39* gene (882-bp product). Amplifications were carried out for 40 cycles at 94°C for 1 min, 54°C for 1 min, and 72°C for 45 s. For PCRs carried out directly with DNase-treated RNA preparations (controls for the presence of baculovirus genomic DNA contamination), aliquots equivalent to those present in the cDNA preparations used for PCR amplification were used as templates.

Titration of BV and electron microscopy. Hz-AM1 cells were infected with the indicated viruses at a multiplicity of infection (MOI) of 0.1. Supernatants were collected at 87 h postinfection (hpi), and cells were dislodged and pelleted at 5,000 × *g* for 5 min. The titers of supernatants were determined by end-point dilution assay with Hz-AM1 cells. Cells collected at 7 days postinfection were fixed, dehydrated, embedded, sectioned, and stained as described previously (21). Samples were viewed with a JEM-1230 transmission electron microscope at an accelerating voltage of 80 kV.

Fluorescence microscopy analysis. Hz-AM1 (1×10^5) cells were grown on glass coverslips in petri dishes and infected with the indicated viruses. For the localization of cellular actin, infected cells were fixed at 60 hpi for 10 min on ice in 2% formaldehyde and 0.2% glutaraldehyde in PBS, washed once with PBS, solubilized with 0.15% Triton X-100, stained with rhodamine-phalloidin (Sigma), and then examined under a Leica S2 laser confocal scanning microscope for fluorescence. vHa-eGFP was used as a control.

Subcellular localization. To detect the localization of HA2 and truncated HA2 fragments in insect cells, pIZ/V5-eGFP-X plasmids ("X" represents empty plasmid or WT or truncated *ha2* fragments), which allow the expression of the N-terminal EGFP fusion protein in Hz-AM1 cells, were constructed. The *egfp* fragment, which was PCR amplified with primers egfp2 forward and egfp2 reverse, with pEGFP-N1 as the template, was inserted into the multicloning region of pIZ/V5 to produce pIZ/V5-eGFP. All of the *ha2* fragments, which were digested from donor plasmids by EcoRI and XhoI, were subcloned into pIZ/V5-eGFP and fused with *egfp*. Hz-AM1 cells (1×10^5) were transfected with these plasmids. By 48 h posttransfection (hpt), cells were fixed, stained with Hoechst (Beyotime), and then examined under a Leica S2 laser confocal scanning microscope for fluorescence. For coinfection experiments, transfected cells were infected with HearNPV G4 at an MOI of 5 at 6 hpt. At 72 hpi, cells were fixed, stained with Hoechst, and then observed under a laser confocal scanning microscope.

RESULTS

Generation of recombinant bacmids. To investigate the function of *ha2* during the viral infection cycle, we constructed an *ha2* knockout bacmid of HearNPV in which the major *ha2* coding sequences were replaced with a *cat* gene cassette and a 579-bp segment of the 5′ end of the *ha2* coding sequence was retained to preserve the *havPK* promoter (Fig. 1A). Knockout of *ha2* was confirmed by PCR (Fig. 1B). PCR products derived with primer pairs CATU/B1 and CATU/CATD from HaΔha2 were 1,039 bp long (Fig. 1C), confirming replacement of *ha2* by the *cat* cassette. In contrast, no signal was detected with the WT control HaBacHZ8. The primer combinations A4/B3 and A5/B1 generated PCR products of 201 bp and 462 bp from HaBacHZ8, but they were unable to amplify PCR products from HaΔha2, indicating the loss of the 663 bp within the *ha2* coding region. Furthermore, PCR analysis of HaΔha2 resulted in products of 1,702 bp and 1,039 bp with primer sets A1/CATD and A4/B1, respectively, while only a 663-bp product was obtained from HaBacHZ8 with primer set A4/B1 and no product was obtained with primer pair A1/CATD. Thus, these data indicated that the *ha2* gene was deleted and replaced with the *cat* cassette by homologous recombination in HaΔha2.

To generate an *ha2* repair bacmid, a transfer plasmid was constructed for transposition into the polyhedrin (*polh*) locus of the *ha2* knockout bacmid HaΔha2. The transfer plasmid pFastBac Dual was first modified by replacing the *polh* promoter with a copy of the *ha2* promoter (nt 1992 to 2082 of HearNPV) (4) and inserting a copy of *egfp* downstream of the *p10* promoter. The *ha2* and truncated *ha2* fragments were then inserted downstream from the *ha2* promoter. The truncated fragments were C129, C170, C194, C261, N193, N260, PWCA, HWCA, and WCA (Fig. 1D). After transposition, the recombinants were confirmed by PCR with the primers M13 forward and gfp1 forward (Table 1) (data not shown). The resulted repair bacmids were named HaΔha2-ha2, HaΔha2-C129, HaΔha2-C170, HaΔha2-C194, HaΔha2-C261, HaΔha2-N193, HaΔha2-N260, HaΔha2-PWCA, HaΔha2-HWCA, and HaΔha2-WCA (Fig. 1D). All of the recombinant bacmids contained *egfp* under the control of the *p10* promoter and *ha2* or truncated *ha2* controlled by the native *ha2* promoter. HaΔha2-eGFP and Ha-eGFP (5, 18) were the negative and positive controls, respectively.

***ha2* is essential for BV production.** The *ha2* null (HaΔha2-eGFP), *ha2* repair (HaΔha2-ha2), and WT control (Ha-eGFP) constructs were used in turn to transfect Hz-AM1 cells. Green fluorescence was detected at 72 hpt, and there was no difference among the three viruses, indicating comparable transfection efficiencies (Fig. 2A). However, fluorescence accumulated in both Ha-eGFP- and HaΔha2-ha2-transfected cells, while HaΔha2-transfected cells showed almost no increase in the number of infected cells (Fig. 2A), indicating that there was no spread of the virus beyond the cells initially transfected with the *ha2* knockout bacmid DNA. When the supernatant was used to infect Hz-AM1 cells, HaΔha2-ha2 could set up infection, while HaΔha2-eGFP did not produce any EGFP at any time points analyzed for up to 168 h (Fig. 2A). These results indicated that *ha2* is essential for infectious BV production.

However, HaΔha2-eGFP could also produce EGFP under

are shown below. (D) Strategy for two recombinant bacmids. Diagrams for Ha-eGFP and HaΔha2-X are given, showing the polyhedrin (*polh*) and *egfp* genes inserted into the polyhedrin locus by Tn*7*-mediated transposition. X is shown in the schematic of the full-length *ha2* and deletion mutants. The designations for the WT *ha2* construct and each mutant are indicated under the "X," and the names of the corresponding recombinant repair bacmids are shown on the left. The sketch map at the top represents the domain structure, and the numbers indicate amino acid positions. The N-terminal domain contains aa 1 to 128, the proline-rich region contains aa 129 to 169, the WCA domain contains aa 194 to 260, the H domain contains aa 170 to 193, and the C-terminal region with PtdIns 4-kinase homology contains aa 261 to 413. Thin lines indicate the coding regions retained in WT *ha2* or truncated mutants. The number at the left or right of each line denotes the starting amino acid or the ending amino acid in each construct. The arrows and the corresponding letters, A1 to A6 and B1 to B3, represent the primers used to amplify these fragments.

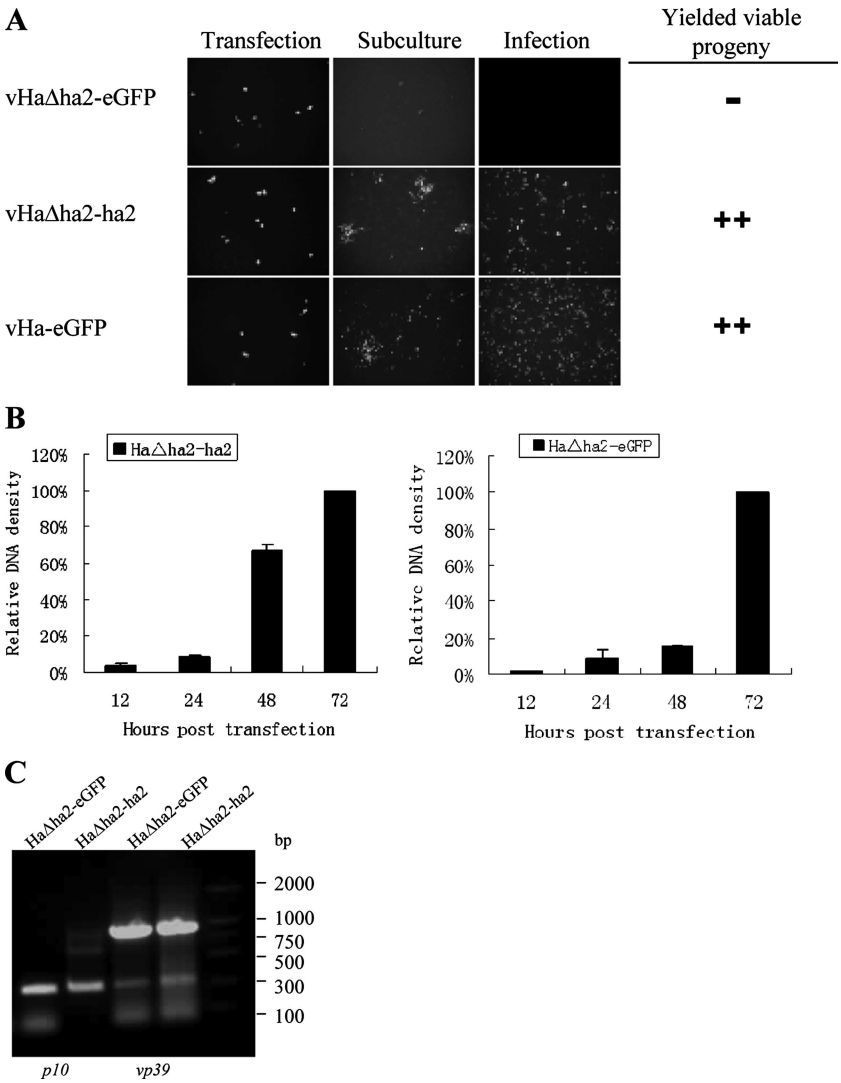

FIG. 2. *ha2* is essential for BV production. (A) Fluorescence microscopy images in the left and middle panels show Hz-AM1 cells (5×10^5) transfected with 2.0 μg of DNA of HaΔha2-eGFP, HaΔha2-ha2, and Ha-eGFP (at 96 hpt) and subcultured at 96 h, respectively. The right panels show new monolayer cells which were infected with the cell culture supernatants of subcultured cells at 96 hpi. The right table is a summary of the viability of progeny by rescue of *ha2*. +, applicable; −, not applicable; each additional + represents a stronger signal. (B) Real-time PCR analysis of viral DNA replication in transfected Hz-AM1 cells. At the designated times, total DNAs were isolated from Hz-AM1 cells transfected with the indicated bacmid constructs, digested with the restriction enzyme DpnI to eliminate input bacmid DNA, and analyzed by real-time PCR using SYBR green I. Values are displayed as averages for transfections performed in triplicate, with error bars indicating standard deviations. (C) Validation of gene expression levels by RT-PCR following HaΔha2-eGFP and HaΔha2-ha2 transfection of Hz-AM1 cells, determined at 96 hpt. RT-PCR was performed for two genes, *p10* and *vp39*, which displayed similar transcriptional efficiencies between control and HaΔha2-eGFP-transfected cells.

the control of the very late gene promoter after transfection, implying that the HaΔha2-eGFP genome could still replicate. Quantitative real-time PCR was performed with DNAs from cells transfected with bacmids, and the results indicated that the *ha2* knockout bacmid was still able to synthesize nascent DNA at 72 hpt, like the *ha2* repair bacmid, suggesting that *ha2* is not involved in viral DNA replication (Fig. 2B).

We next analyzed the RNA content at 96 hpt of Hz-AM1 cells transfected with HaΔha2-eGFP and HaΔha2-ha2, using RT-PCR. As shown in Fig. 2C, the presence of transcripts originating from *vp39* and *p10* in both HaΔha2-eGFP- and HaΔha2-ha2-transfected cells demonstrated that transcription of the late and very late viral genes was not blocked by the lack of *ha2*.

The WCA domain of HA2 accelerates Arp2/3-mediated actin assembly in vitro. Transfection and infection analysis demonstrated that not only the entire *ha2* gene rescued the infectious BV production defect, but some retrieved truncated *ha2* fragments, including C129, C170, N260, PWCA, and HWCA (Fig. 3A), all of which contained the WCA domain (Fig. 1D), also did so. The other recombinants, vHaΔha2-C194′vHaΔha2-C261 and vHaΔha2-N193, did not yield progeny upon infection (Fig. 3A). These results demonstrate that the WCA domain is essential for viral replication. The WCA domain of HA2 is a

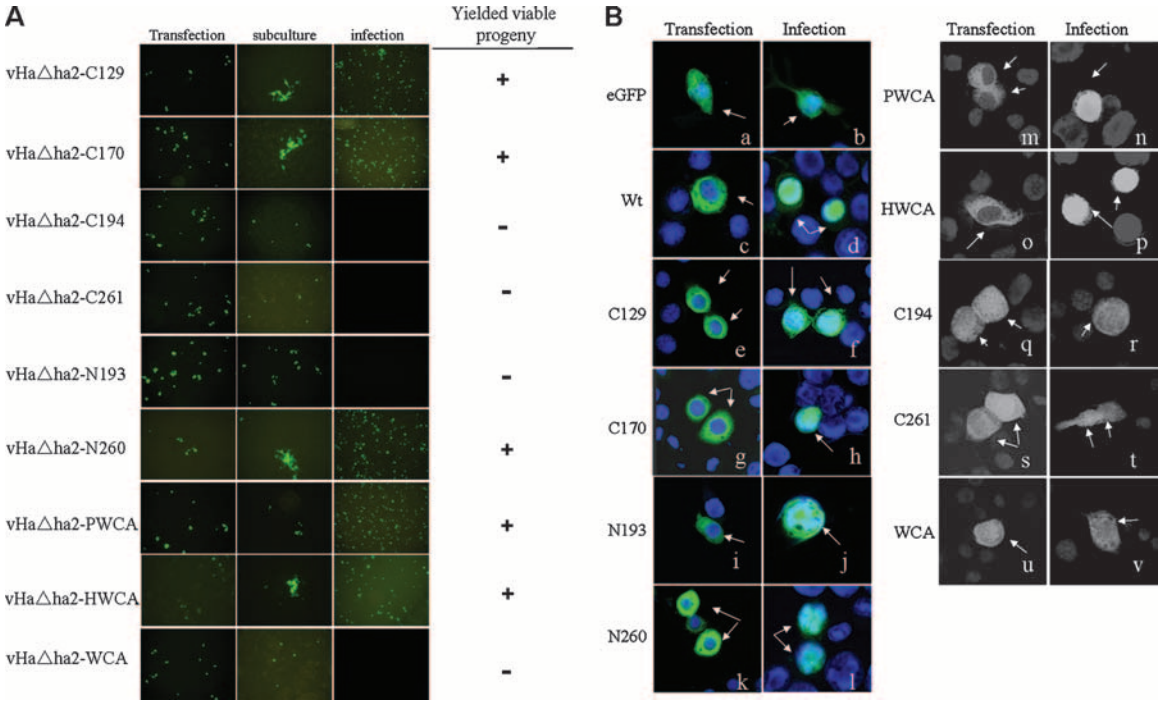

FIG. 3. The hydrophobic domain (aa 167 to 193) plays a pivotal role in BV production and the localization/transportation of HA2. (A) Fluorescence microscopy images of the left and middle panels show Hz-AM1 cells (5×10^5) transfected with 2.0 μg of DNA of HaΔha2-C129, HaΔha2-C170, HaΔha2-C194, HaΔha2-C261, HaΔha2-N193, HaΔha22-N260, HaΔha2-PWCA, HaΔha2-HWCA, and HaΔha2-WCA (at 96 hpt) and subcultured at 96 h, respectively. The right panels show new monolayer cells which were infected with the cell culture supernatants of subcultured cells or lymph of injected larvae at 96 hpi. The right table is a summary of the viability of progeny by rescue with a series of truncated mutants. (B) Hz-AM1 cells grown on glass coverslips were transfected with EGFP vector, HA2 expressed from a plasmid as a fusion with EGFP, or plasmid constructs in which all fragments were fused in frame to EGFP (left panels). Six hours after transfection, cells were infected with virus HearNPV strain G4 (MOI, 5) (right panels). Cells were fixed with 4% paraformaldehyde, and DNA in the nucleus was stained with Hoechst (500 μl/10^6 cells) 48 h after transfection or 72 h after infection and then visualized by indirect fluorescence microscopy analysis of EGFP. The results shown are overlaid images indicating the superimposed signals of EGFP (green) and Hoechst staining (blue). Arrows denote the corresponding cells transfected with plasmid constructs. The designations for WT *ha2*, EGFP, and mutant fragments are indicated on the left.

conservative motif of the WASP family, which includes the G-actin-binding (WH2) domain, a cofilin homology sequence (C), and an acidic segment (A). These sequences have been shown to be necessary and sufficient for activating the Arp2/3 complex (9, 16). For in vitro analysis, we expressed and purified His fusion proteins containing the WCA, WC, or CA domain and first tested their ability to interact with actin in a pull-down assay. Actin bound to His-WC and His-WCA but not to His-CA (data not shown), indicating that WH2 is an actin-binding domain in HA2 (22). We then tested the ability to activate actin polymerization and found that the His-WCA fusion protein together with the Arp2/3 complex accelerated assembly, increased the elongation rate, and shortened but did not eliminate the lag phase, while the WC and CA fusions had almost no activity (data not shown) (9). Compared to full-length HA2, the His-WCA fragment was just as effective in stimulating actin polymerization.

A hydrophobic domain plays a pivotal role in localization/transportation of HA2. To our surprise, vHaΔha2-WCA, which contained the minimal WCA domain, could not produce infectious particles. Comparison of vHaΔha2-HWCA with vHaΔha2-WCA revealed that the insertion of vHaΔha2-HWCA had an extra 27 aa (aa 167 to 193) over the WCA domain, suggesting that this sequence played an important role in rescuing the defect of the knockout of *ha2* associated with the WCA domain. Sequence analysis indicated that aa 167 to 193 were highly hydrophobic, and we therefore named the region the H domain.

It has been demonstrated that hydrophobic domains of baculoviral structural proteins, such as AcMNPV ODV-E66 and PIF-3, function as sorting motifs to transport fusion proteins to the nucleus and virions (10, 13). The results shown in Fig. 3B indicate that the distribution of EGFP-HA2 transiently expressed by plasmid was within the cytoplasm (panel c), while the EGFP control was diffused throughout the cells (panel a). The truncated *ha2* fragments, including C129, C170, C194, C261, N193, N260, PWCA, HWCA, and WCA, were tagged with EGFP at the carboxyl terminus, and these recombinant plasmids were transfected into Hz-AM1 cells. Consistent with the full-length EGFP-HA2 fusion protein, C129 (Fig. 3B, panel e), C170 (Fig. 3B, panel g), N193 (Fig. 3B, panel i), N260 (Fig. 3B, panel k), PWCA (Fig. 3B, panel m), and HWCA (Fig. 3B, panel o) were preferentially localized in the cytoplasm, and no obvious nuclear accumulation was observed in over 90% of cells transfected. However, the remaining mutants, C194 (Fig. 3B, panel q), C261 (Fig. 3B, panel s), and WCA (Fig. 3B, panel u), spread throughout the whole cell, showing a similar distribution pattern to that observed in cells transfected with pIZ/

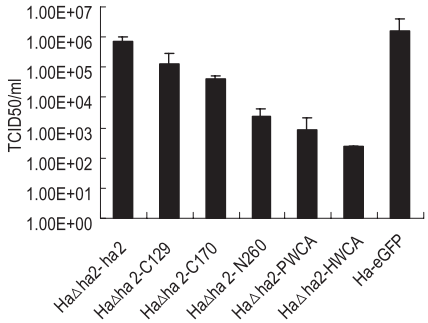

FIG. 4. Infectivity of repair recombinant HearNPVs. Cells (5×10^5) were infected with each virus at an MOI of 0.1, and the cell culture supernatants were harvested at 87 hpi and assayed for the production of infectious virus by $TCID_{50}$ assay. Each data point represents the average titer derived from two independent $TCID_{50}$ assays. Error bars represent standard errors.

V5-eGFP; this was probably due to passive diffusion. After superinfection of HearNPV, the EGFP-HA2 fusion protein was transported from the cytoplasm into the nucleus (Fig. 3B, panel d), while EGFP alone was present throughout the whole cells all the time (Fig. 3B, panel b), as previously reported (5, 18). The truncated fragments C129 (Fig. 3B, panel f), C170 (Fig. 3B, panel h), N193 (Fig. 3B, panel j), N260 (Fig. 3B, panel l), PWCA (Fig. 3B, panel n), and HWCA (Fig. 3B, panel p), all of which were localized in the cytoplasm of the transfected cells, exhibited similar distribution patterns to that of full-length HA2 after infection with virus and were also transported into the nucleus. However, mutants C194 (Fig. 3B, panel r), C261 (Fig. 3B, panel t), and WCA (Fig. 3B, panel v) appeared to display the same distribution as EGFP alone and remained present throughout the whole cell after infection with virus. These results indicated that HA2 itself localizes in the cytoplasm and is recruited to the nucleus with the help of a viral factor(s) and that the H motif (aa 167 to s193) is essential for the localization and translocation of HA2.

Infectivity of recombinant repair HearNPVs. To further assess the infectivity and BV production of the recombinant HearNPVs, Hz-AM1 cells were synchronously infected with BV of the recombinant viruses and the titers were determined by an end-point dilution assay at 87 hpi. The titers of vHaΔha2-ha2 and vHa-eGFP were about 1.8×10^6 and 4×10^6 50% tissue culture infective doses ($TCID_{50}$)/ml, respectively, which were not significantly different (Fig. 4). The mutants succeeding in rescuing the defect of infectious BV production showed delayed viral production and reduced titers. vHaΔha2-C129 and vHaΔha2-C170 produced only 3.2×10^5 and 1.1×10^5 $TCID_{50}$/ml, indicating that deleting the N terminus, including the proline-rich region, decreased the infectivity of the recombinant. Moreover, the deletion of C-terminal region PtdIns 4-kinase homology dramatically decreased the production of BV, as the titers of HaΔha2N260, HaΔha2-PWCA, and HaΔha2-HWCA were only 4.6×10^3, 2.2×10^3, and 0.6×10^3 $TCID_{50}$/ml, respectively, which were about 1,000-fold lower than those of vHaΔha2-ha2 and vHa-eGFP (Fig. 4). Thus, the C terminus of HA2 is significant for high-efficiency BV yields.

HA2 is involved in virion assembly. The titer results described above indicated that there could be some defect in BV production of the repaired viruses with truncated *ha2* fragments. To further analyze whether the different domains affect nucleocapsid structure, electron microscopy was performed with virus-infected cells at 87 hpi (Fig. 5). Both WT and *ha2* repair viruses produced characteristic normal occluded virions

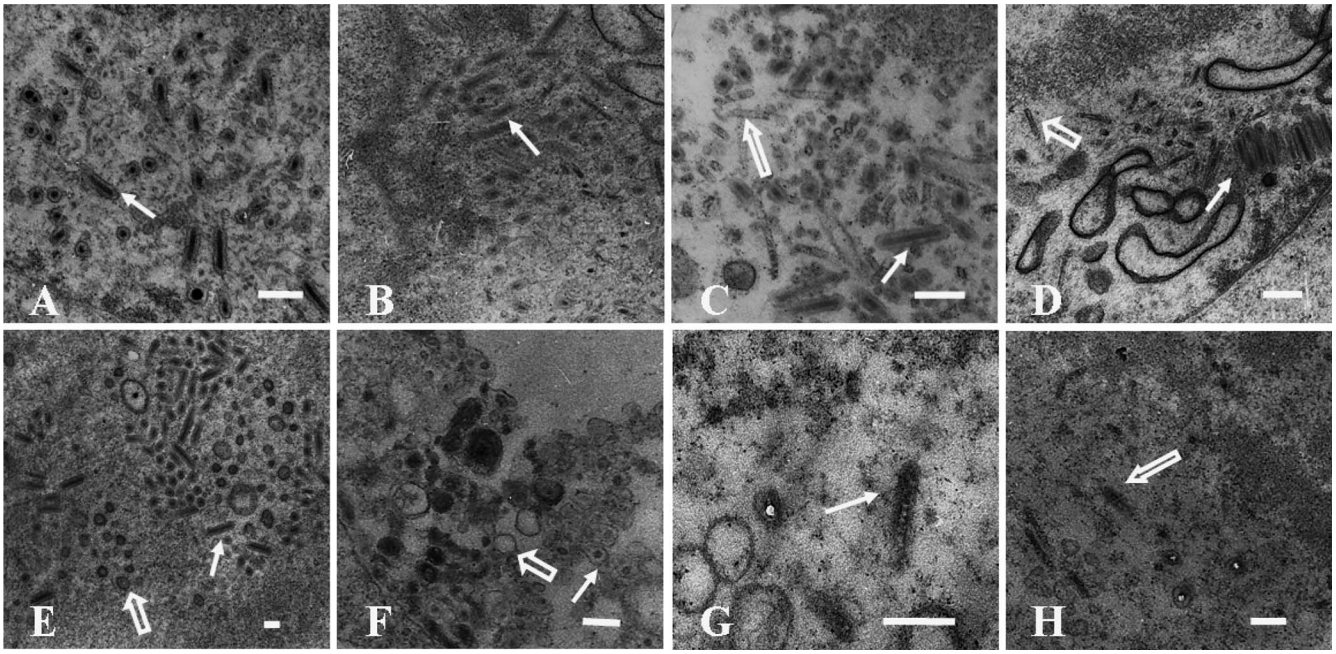

FIG. 5. HA2 is involved in virion assembly. Portions of cells infected with vHa-eGFP (A), vHaΔha2-ha2 (B), vHaΔha2-C129 (C), vHaΔha2-C170 (D), vHaΔha2-N260 (E), vHaΔha2-PWCA (F), and vHaΔha2-HWCA (G and H) are shown. Solid arrows denote normal nucleocapsids; open arrows denote abnormal ones. Bar, 200 nm.

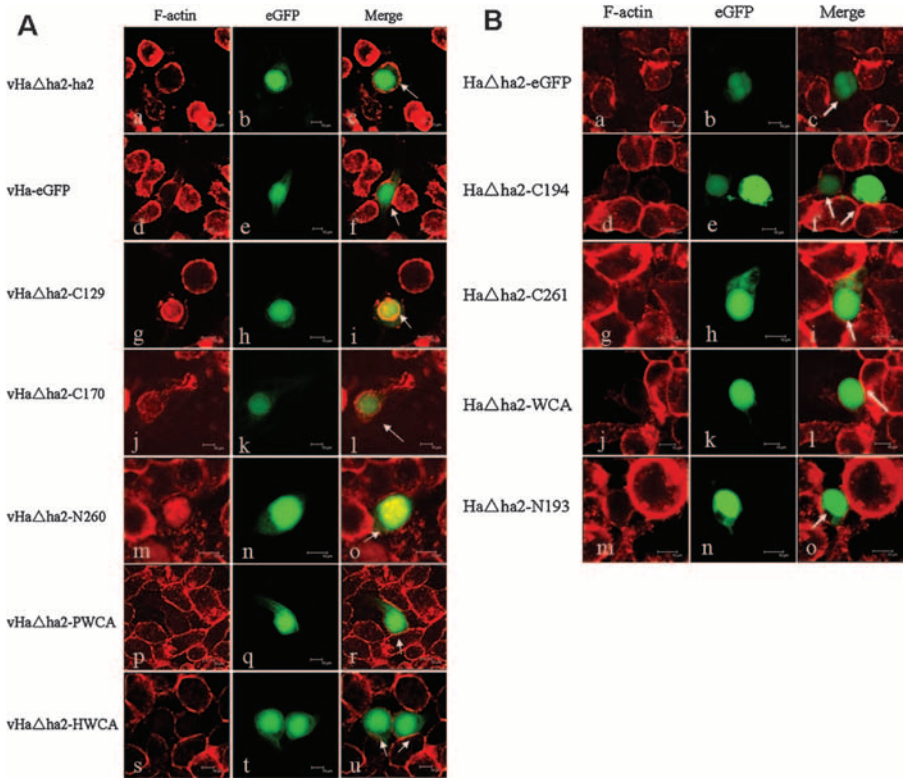

FIG. 6. Actin kinetics in HaΔha2-X-infected cells. (A) Fluorescence microscopy images in the left and middle panels show Hz-AM1 cells (5×10^5) infected with vHaΔha2-eGFP, vHaΔha2-ha2, vHa-eGFP, vHaΔha2-C129, vHaΔha2-C170, vHaΔha2-N260 vHaΔha2-PWCA, and vHaΔha2-HWCA. All cells were fixed, and microfilaments were labeled with rhodamine-phalloidin (left panels). Overlaid images indicate the superimposed signals of infected cells and phalloidin staining (right panels). Arrows denote the corresponding cells infected with the indicated virus. (B) Hz-AM1 cells (5×10^5) were transfected with vHaΔha2-eGFP, vHaΔha2-C194, vHaΔha2-C261, vHaΔha2-N193, and vHaΔha2-WCA (middle panels). Fluorescence microscopy images in the left panels show the microfilament distribution. The right panels are the merged images. Bar, 10 nm.

containing single nucleocapsids and surrounded by tight membranous envelopes (Fig. 5A and B). Compared to the WT, vHaΔha2-C129 could also form many obvious typical nucleocapsids, but there still existed some abnormal structures. Some electron-lucent tubular structures were dispersed in the nucleus, indicating that they lack an electron-dense core, which would be indicative of nucleoprotein (Fig. 5C). vHaΔha2-C170 had the same result (Fig. 5D). We also observed apparent defects in vHaΔha2-N260-infected cells, and there were abundant membranes without associated nucleocapsids and the same electron-lucent tubular structures (Fig. 5E). Besides a few normal virions, vHaΔha2-PWCA also formed a mass of free membranes without nucleocapsids (Fig. 5F). In vHaΔha2-HWCA-infected cells, normal occluded virions were very hard to find, and there was an abundance of electron-lucent tubular structures and some hollow tubular structure which probably lacked both envelopes and electron-dense core (Fig. 5G and H).

Actin kinetics in HaΔha2-X-infected cells. Nuclear F-actin is essential for baculovirus infection (20, 25), and the baculoviral WASP-like protein activates dynamic actin polymerization in the nucleus to enable viral replication and nucleocapsid morphogenesis (18, 28). Changes of the actin cytoskeleton were analyzed during the infection of Hz-AM1 cells by different repair viruses (Fig. 6A). In vHaΔha2-ha2- and vHa-eGFP-infected cells, F-actin aggregated at the plasma membrane during the early stage of infection and then appeared within the nucleus (data not shown), and finally, microfilaments were transported to the cytoplasm and plasma membrane, again at a very late stage of infection (Fig. 6A, panels a to c and d to f), which agreed with the result that F-actin is transported from the cytoplasm into the nucleus and then out of it in the very late phase of baculovirus infection (7, 14, 19). Cells infected with vHaΔha2-C129, vHaΔha2-C170, and vHaΔha2-N260 had a dramatically different configuration of microfilaments, which were located in the nucleus until 60 hpi. F-actin appeared within the nucleus and, more prominently, within the surrounding "ring zone" after Hz-AM1 cells were infected with vHaΔha2-C129 by 60 hpi (Fig. 6A, panels g to i). In cells infected by vHaΔha2-C170, microfilaments in the nucleus were localized in the peripheral to the virogenic stroma (Fig. 6A, panels j to l). Phalloidin labeling of microfilaments in vHaΔha2-N260-infected cells showed a fine homogeneous network within the central virogenic stroma of the nucleus or the whole nucleus (Fig. 6A, panels m to o). vHaΔha2-PWCA- and vHaΔha2-HWCA-infected cells showed microfilaments with small amounts of F-actin aggregated in the plasma membrane (Fig. 6A, panels p to r and s to u). The different subcellular localizations of F-actin in the cells infected with different recombinants implied that they were at different replication stages. Moreover, Hz-AM1 cells which were transfected with viruses HaΔha2-eGFP (Fig. 6B, panels a to c), HaΔha2-C194

(Fig. 6B, panels d to f), HaΔha2-C261 (Fig. 6B, panels g to i), HaΔha2-WCA (Fig. 6B, panels j to l), and HaΔha2-N193 (Fig. 6B, panels m to o), which could not produce infectious BV, exhibited microfilaments with little F-actin localized in either the plasma or nucleus.

DISCUSSION

Baculovirus WASP proteins, such as AcMNPV P78/83 and HearNPV HA2, are activators that direct actin polymerization-based motility of virions and further demonstrate that F-actin-dependent progeny morphogenesis appears to be a characteristic common to viruses that have lepidopteran hosts (12). A *ha2* knockout bacmid revealed a phenotype that was unable to produce BV. This defect could be rescued by the repair of *ha2*, and the repaired virus was equivalent to the WT with respect to replication in host cells, indicating that *ha2* was required for production of infectious BV. Quantitative real-time PCR results determined that the deletion of *ha2* did not affect viral DNA replication and the transcription of the viral late and very late genes, suggesting that the defect of virus morphogenesis might be related to the assembly of the virus. In AcMNPV, the deletion of P78/83, an HA2 homologue, also leads to the defect in yielding progeny (9).

Electron microscopy performed on *ha2* and truncated fragment repair viruses demonstrated that the lower efficiency of production of BV might be due to a defect in nucleocapsid assembly. The full-length repair virus produced a typical occluded virus, like the WT virus did. However, we observed virus assembly defects in the truncated *ha2* fragment repair viruses. Together with the results of infectivity assays, the lower the titration was, the greater was the defect in virion organization. It has been reported that long tubular structures largely devoid of viral DNA are located primarily in the nucleus and are associated with the inner nuclear membrane of AcMNPV-infected cells in the presence of cytochalasin D (25). Excessively long tubular structures were located primarily in the nuclei of these truncated viruses, suggesting that these observations might be due to interference with the assembly of normal capsids by blocking the polymerization of F-actin, which is consistent with the observation of F-actin localization in these virus-infected cells. The abundance of membranes without associated nucleocapsids in vHaΔha2-PWCA-infected cells and of hollow tubular structures in vHaΔha2-HWCA-infected cells further indicated that nuclear actin polymerization is coordinated with nucleocapsid morphogenesis and membrane-capsid interactions during virion assembly (9). Our observations with mutant virus-infected cells were similar to those detected in p78/83 point mutant AcMNPV-transfected cells. It seems that lepidopteran NPVs probably use the same mechanism for nuclear actin polymerization to facilitate virus assembly in the nucleus and virus morphogenesis (9).

Four stages of actin rearrangement have been distinguished in AcMNPV-infected cells. After actin cables are detected within the cytoplasm, the formation of F-actin aggregates at the plasma membrane occurs at the early stage of infection (7). F-actin then appears within the nucleus, and finally, microfilaments are transported to the cytoplasm and plasma membrane once again (19). The distribution of F-actin in vHaΔha2-ha2- and vHa-eGFP-infected cells showed that they were in the very late stage of infection at 87 hpi. However, the presence of F-actin suggested that vHaΔha2-C129, vHaΔha2-C170, and vHaΔha2-N260 might be in the late stage of infection at 87 hpi. Compared to the WT, these three viruses showed a delay of propagation which might be due to the retarding of actin assembly and further confirmed the lower efficiency of the BV titer. The quite different localization of F-actin in vHaΔha2-PWCA- and vHaΔha2-HWCA-infected cells pointed to a hypothesis that in these cases, it was difficult to recruit and polymerize F-actin in the nucleus, which would further affect the assembly of the virus. Those viruses which could not yield viable progeny might be the result of defects in nuclear actin assembly (9).

Sequence alignments indicate that HA2 contains motifs, such as the proline-rich region and the WCA domain, which are common to WASP or WASP-like proteins. The WCA domain of the HA2 fragment is able to interact with actin directly in vitro, and the WH2 domain is a G-actin-binding site, which is consistent with observations for Scar1/WAVE and WASP (16). In addition, the WCA domain is the minimal functional unit of HA2 necessary to activate the Arp2/3 complex and has a similar effect on actin polymerization kinetics (data not shown). Based on these findings, and combined with those reported from the observation of AcMPNV P78/83 (9), we conclude that WCA of the baculoviral WASP also appears to stimulate actin polymerization via the Arp2/3 complex.

However, the WCA region is essential but not enough to rescue the defective phenotype of the *ha2* knockout. Comparing the truncated fragments in infectious viruses, we found that the repaired fragment in vHaΔha2-HWCA is the shortest one that contains the WCA domain and a 27-aa sequence (aa 167 to 193) which predominantly comprises hydrophobic amino acids such as leucine, isoleucine, and valine. Subcellular location analysis of different truncated fragments indicated that this motif might be a nuclear localization signal or sorting motif (Fig. 5) similar to that found in baculoviral structural proteins, such as AcMNPV ODV-E66, and the PIF-3 hydrophobic domain responsible for trafficking of fusion protein to the nucleus and virion (10, 13). However, unlike the sorting motif domain of ODV-E66, which is sufficient to traffic fusion proteins to the inner nuclear membrane and the ODV envelope with an efficiency similar to that of the WT protein (2), HA2 requires another viral factor(s) for efficient transportation from the cytoplasm to the nucleus, as reported for PIF-3 (13). Sequence BLAST results showed that there existed no homologous motif in the other *ha2* homologues of lepidopteran baculoviruses. However, the sequence between the proline-rich and WCA domains is usually rich in hydrophobic amino acids, which might endow it with a conserved function.

PtdIns 4-kinase functions in the Pkc1-mediated mitogen-activated protein (MAP) kinase cascade, and a distinct pool of PI4P generated by PtdIns 4-kinase is critical for normal actin cytoskeleton organization (1). In the C terminus of HA2, there is an exclusive domain homologous to PtdIns 4-kinase which has not been reported for any WASP family protein to date. Interestingly, the deletion of the C terminus resulted in a dramatic decrease of virus infectivity. Compared to the WT, the BV titers of vHaΔha2-N260, vHaΔha2-PWCA, and vHaΔha2-HWCA were reduced almost 1,000 times. Although the C terminus of HA2 was not required for activating the

Arp2/3 complex or inducing actin polymerization, it is significant for a high efficiency of BV production. Further experiments will be performed to clarify its function.

In summary, we have demonstrated that the HA2 WCA region is required for actin polymerization by the Arp2/3 complex in vitro and for infectious virus assembly and production. At the C terminus, a PtdIns 4-kinase homology region is important for increasing the efficiency of BV progeny. The H motif of aa 167 to 193 is essential for the distribution and transportation of HA2. Although the exact roles for some motifs in BV generation are unclear, our results give us a hint about the subcellular localization and elementary function of the HA2 domain in viral replication. Experiments are currently under way to determine how the HA2 domains work in virus morphogenesis.

ACKNOWLEDGMENTS

We are grateful to Simon Rayner and Li Lulin for critical reviews of the manuscript.

This work was supported by the National Nature Science Foundations of China (30325002 and 30470075) and the National Basic Research Program of China (2003CB1140).

REFERENCES

1. **Audhya, A., and S. D. Emr.** 2002. Stt4 PI 4-kinase localizes to the plasma membrane and functions in the Pkc1-mediated MAP kinase cascade. Dev. Cell **2:**593–605.
2. **Braunagel, S. C., S. T. Williamson, S. Saksena, Z. Zhong, W. K. Russell, D. H. Russell, and M. D. Summers.** 2004. Trafficking of ODV-E66 is mediated via a sorting motif and other viral proteins: facilitated trafficking to the inner nuclear membrane. Proc. Natl. Acad. Sci. USA **101:**8372–8377.
3. **Charlton, C. A., and L. E. Volkman.** 1991. Sequential rearrangement and nuclear polymerization of actin in baculovirus-infected *Spodoptera frugiperda* cells. J. Virol. **65:**1219–1227.
4. **Chen, X., W. IJkel, R. Tarchini, X. Sun, H. Sandbrink, H. Wang, S. Peters, D. Zuidema, R. K. Lankhorst, J. M. Vlak, and Z. Hu.** 2001. The sequence of the *Helicoverpa armigera* single nucleocapsid nucleopolyhedrovirus genome. J. Gen. Virol. **82:**241–257.
5. **Chen, X., X. Sun, Z. Hu, M. Li, D. R. O'Reilly, D. Zuidema, and J. M. Vlak.** 2000. Genetic engineering of *Helicoverpa armigera* single-nucleocapsid nucleopolyhedrovirus as an improved pesticide. J. Invertebr. Pathol. **76:**140–146.
6. **Datsenko, K. A., and B. L. Wanner.** 2000. One-step inactivation of chromosomal genes in *Escherichia coli* K-12 using PCR products. Proc. Natl. Acad. Sci. USA **97:**6640–6645.
7. **Dreschers, S., R. Roncarati, and D. Knebel-Morsdorf.** 2001. Actin rearrangement-inducing factor of baculoviruses is tyrosine phosphorylated and colocalizes to F-actin at the plasma membrane. J. Virol. **75:**3771–3778.
8. **Goldberg, M. B.** 2001. Actin-based motility of intracellular microbial pathogens. Microbiol. Mol. Biol. Rev. **65:**595–626.
9. **Goley, E. D., T. Ohkawa, J. Mancuso, J. B. Woodruff, J. A. D'Alessio, W. Z. Cande, L. E. Volkman, and M. D. Welch.** 2006. Dynamic nuclear actin assembly by Arp2/3 complex and a baculovirus WASP-like protein. Science **314:**464–467.
10. **Hong, T., M. D. Summers, and S. C. Braunagel.** 1997. N-terminal sequences from *Autographa californica* nuclear polyhedrosis virus envelope proteins ODV-E66 and ODV-E25 are sufficient to direct reporter proteins to the nuclear envelope, intranuclear microvesicles and the envelope of occlusion derived virus. Proc. Natl. Acad. Sci. USA **94:**4050–4055.
11. **Hou, S., X. Chen, H. Wang, M. Tao, and Z. Hu.** 2002. Efficient method to generate homologous recombinant baculovirus genomes in *E. coli*. BioTechniques **32:**783–788.
12. **Kasman, L. M., and L. E. Volkman.** 2000. Filamentous actin is required for lepidopteran nucleopolyhedrovirus progeny production. J. Gen. Virol. **81:**1881–1888.
13. **Li, X., J. Song, T. Jiang, C. Liang, and X. Chen.** 2007. The N-terminal hydrophobic sequence of *Autographa californica* nucleopolyhedrovirus PIF-3 is essential for oral infection. Arch. Virol. **152:**1851–1858.
14. **Li, X. Q., R. Zhou, Y. L. Jia, F. Jia, Z. H. Yu, and X. Chen.** 2004. Function of actin in transportation of the AcMNPV from nuclear to outside of cell. Virol. Sin. **19:**632–635.
15. **Luckow, V. A., S. C. Lee, G. F. Barry, and P. O. Olins.** 1993. Efficient generation of infectious recombinant baculoviruses by site-specific transposon-mediated insertion of foreign genes into a baculovirus genome propagated in *Escherichia coli*. J. Virol. **67:**4566–4579.
16. **Machesky, L. M., and R. H. Insall.** 1998. Scar1 and the related Wiskott-Aldrich syndrome protein, WASP, regulate the actin cytoskeleton through the Arp2/3 complex. Curr. Biol. **8:**1347–1356.
17. **Machesky, L. M., R. H. Insall, and L. E. Volkman.** 2001. WASP homology sequences in baculoviruses. Trends Cell Biol. **11:**286–287.
18. **Nie, Y., Q. Wang, C. Liang, M. Fang, Z. Yu, and X. Chen.** 2006. Characterization of ORF2 and its encoded protein of the *Helicoverpa armigera* nucleopolyhedrovirus. Virus Res. **116:**129–135.
19. **Ohkawa, T., A. R. Rowe, and L. E. Volkman.** 2002. Identification of six *Autographa californica* multicapsid nucleopolyhedrovirus early genes that mediate nuclear localization of G-actin. J. Virol. **76:**12281–12289.
20. **Ohkawa, T., and L. E. Volkman.** 1999. Nuclear F-actin is required for AcMNPV nucleocapsid morphogenesis. Virology **264:**1–4.
21. **O'Reilly, D. R., L. K. Miller, and V. A. Luckow.** 1992. Baculovirus expression vectors: a laboratory manual. Oxford University Press, New York, NY.
22. **Rohatgi, R., L. Ma, H. Miki, M. Lopez, T. Kirchhausen, T. Takenawa, and M. W. Kirschner.** 1999. The interaction between N-WASP and the Arp2/3 complex links Cdc42-dependent signals to actin assembly. Cell **97:**221–231.
23. **Takenawa, T., and H. Miki.** 2001. WASP and WAVE family proteins: key molecules for rapid rearrangement of cortical actin filaments and cell movement. J. Cell Sci. **114:**1801–1809.
24. **Vanarsdall, A. L., K. Okano, and G. F. Rohrmann.** 2005. Characterization of the replication of a baculovirus mutant lacking the DNA polymerase gene. Virology **331:**175–180.
25. **Volkman, L. E.** 1988. *Autographa californica* MNPV nucleocapsid assembly: inhibition by cytochalasin D. Virology **163:**547–553.
26. **Volkman, L. E., P. A. Goldsmith, and R. T. Hess.** 1987. Evidence for microfilament involvement in budded *Autographa californica* nuclear polyhedrosis virus production. Virology **156:**32–39.
27. **Wang, H., F. Deng, G. P. Pijlman, X. Chen, X. Sun, J. M. Vlak, and Z. Hu.** 2003. Cloning of biologically active genomes from a *Helicoverpa armigera* single-nucleocapsid nucleopolyhedrovirus isolate by using a bacterial artificial chromosome. Virus Res. **97:**57–63.
28. **Wang, Q., C. Liang, J. Song, and X. Chen.** 2007. HA2 from the *Helicoverpa armigera* nucleopolyhedrovirus: a WASP-related protein that activates Arp2/3-induced actin filament formation. Virus Res. **127:**81–87.
29. **Yamaguchi, H., H. Miki, S. Suetsugu, L. Ma, M. W. Kirschner, and T. Takenawa.** 2000. Two tandem verprolin homology domains are necessary for a strong activation of Arp2/3 complex-induced actin polymerization and induction of microspike formation by N-WASP. Proc. Natl. Acad. Sci. USA **97:**12631–12636.